Chemical Physics 36 (1979) 15–26

ELECTRONIC PROPERTIES OF THE TRIPLET STATE OF FLUORENE, CARBAZOLE, DIBENZOFURAN AND DIBENZOTHIOPHENE (X-TRAPS)

W. GOLDACKER, D. SCHWEITZER and H. ZIMMERMANN
Max-Planck-Institut, Abteilung für Molekulare Physik, 6900 Heidelberg, Germany

Received 11 August 1978

The triplet state of X-traps in neat single crystals of fluorene, carbazole, dibenzofuran and dibenzothiophene was investigated by the method of ODMR in zero field at 1.3 K. In addition to the intersystem crossing rates, steady state populations, decay rate constants and relative radiative rate constants of the sublevels, the spin–lattice relaxation (SLR)-rates were measured, which could not be neglected even at this low temperature. In the case of dibenzothiophene a strong intramolecular heavy-atom effect due to the sulphur atom was observed which allowed direct $S_0 \rightarrow T_1$ excitation.

1. Introduction

A common method to obtain information about electronic properties of excited molecules are optical investigations of shallow X-traps in molecular crystals. X-traps are molecules in the crystal lattice which are slightly disturbed. The disturbancy may for instance originate from impurities with energetically higher electronic states with respect to the crystal molecules, from lattice imperfections or from isotopically different molecules. Impurity induced X-traps in the excited singlet state in crystals of naphthalene were first investigated by Proepstl and Wolf [1]. The triplet state of naphthalene-h_8 in naphthalene-d_8 crystals investigated by Schwoerer and Wolf [2] using ESR is a typical example of traps in isotopically mixed systems.

In the case of molecular crystals of high purity the commonly observed shallow X-traps originate from lattice imperfections such as dislocations or other defects, or from isotopically different molecules due to the different natural abundance of the nuclei [3]. In this paper we report on investigations of the triplet state of X-traps in neat single crystals of fluorene, carbazole, dibenzofuran and dibenzothiophene. The molecular structures of these compounds are very similar, see fig. 1. We were mainly interested in the parameters characterizing the dynamic behaviour of the triplet states such as intersystem crossing rates, steady state populations, decay rate constants and relative radiative rate constants of the sublevels. A strong influence of the intramolecular heavy-atom effect on these dynamic properties due to the sulphur atom was expected for dibenzothiophene.

The method of optical detection of magnetic resonance (ODMR) in zero field at low temperatures was used for these studies. A difficulty we encountered was the fact that spin–lattice relaxation (SLR) between the triplet sublevels could not be suppressed even by lowering the temperature to 1.3 K, except for dibenzothiophene.

The similarity of the four molecules is reflected in the crystal structures as well. Fluorene, carbazole and dibenzofuran crystallize in orthorhombic form (D_{2h}) [4–6] while dibenzothiophene crystals are monoclinic [7]. In all four cases the unit cell contains four mole-

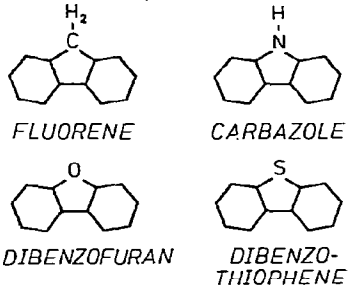

Fig. 1. Molecules: fluorene, carbazole, dibenzofuran and dibenzothiophene.

Table 1
Crystal data of fluorene, carbazole, dibenzofuran and dibenzothiophene

		Ref.	Space group	Z	a (Å)	b (Å)	c (Å)	β
fluorene	$C_{13}H_{10}$	[4]	orthorhombic $P_{nam}(D_{2h}^{16})$	4	8.49	5.721	18.97	–
carbazole	$C_{12}H_9N$	[5]	orthorhombic $P_{nam}(D_{2h}^{16})$	4	7.82	5.76	19.32	–
dibenzofuran	$C_{12}H_8O$	[6]	orthorhombic $P_{nam}(D_{2h}^{16})$	4	7.702	5.825	19.185	–
dibenzothiophene	$C_{12}H_8S$	[7]	monoclinic $P\,2_1/c$ (C_{2h}^5)	4	8.67	6.00	18.7	113.9°

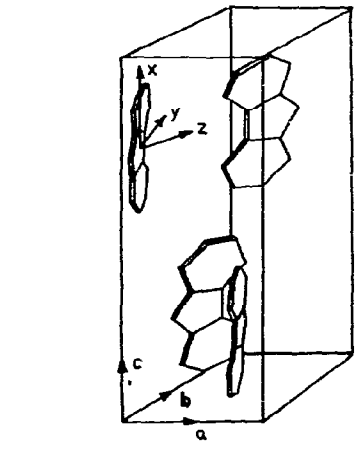

(a)

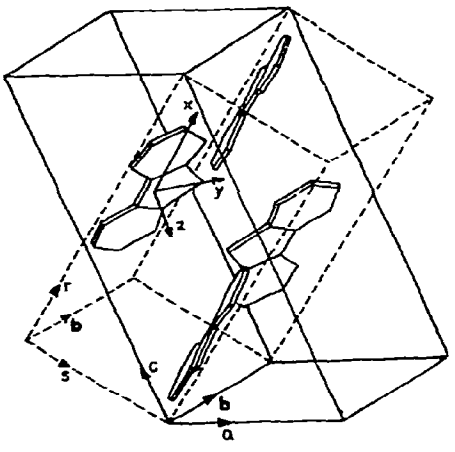

(b)

Fig. 2(a). Unit cells of fluorene-, carbazole- and dibenzofuran-crystals. (b) Unit cell of dibenzothiophene crystals. The principal extinction directions (r, b, s) are shown as well [7].

cules. Table 1 shows the condensed crystal data. The unit cell of fluorene, carbazole or dibenzofuran is drawn in fig. 2a while the one of dibenzothiophene is shown in fig. 2b. In fig. 2b the principal extinction directions (*r*,*b*,*s*) are drawn as well [7]. With respect to these directions all four molecules – including dibenzothiophene – are arranged in a similar manner.

Electronic spectra of fluorene, carbazole, dibenzofuran and dibenzothiophene were studied by several authors. Bree and Zwarich [8] investigated singlet and triplet emission spectra of impurity (dibenzothiophene) induced X-traps in fluorene crystals. The electronic states of carbazole were investigated in several papers [9–11], whereby Haink and Huber [10] show fluorescence and phosphorescence spectra of carbazole in *n*-heptane. Electronic spectra of dibenzofuran were studied in refs. [11–14] and of dibenzothiophene by Bree and Zwarich [15]. Impurity (dibenzothiophene) induced X-traps in fluorene were investigated with ESR by Sixl and Wolf [16] and with ENDOR by Zimmermann et al. [17,18]. ESR studies of X-traps in pure crystals of fluorene, carbazole and dibenzofuran were carried out by Behnke [19]. He could show that in contrast to the impurity induced X-traps in fluorene [17] the CH_2 protons in the X-traps of pure fluorene crystals have equal bonding angle [19] and are equivalent. This demonstrates the different nature of X-traps in pure crystals which are probably due to lattice imperfections with respect to impurity induced X-traps.

2. Experimental

In order to reduce the impurity level as far as possible, we used synthesized fluorene, carbazole, dibenzo-

furan and dibenzothiophene and not commercial products which are usually isolated from tar. They contain impurities which cannot be removed even by extensive zone refining. The synthesis of these hydrocarbons and the determination of the impurity concentration is described in the appendix. Crystals were grown by the Bridgman method from the melt. For the measurements of the phosphorescence spectra the samples were placed in a liquid He-dewar and the temperature was reduced to 1.3 K by pumping. The crystals were excited with a 250 W mercury lamp, filtered with a 1/4 m Schoeffel-monochromator and additional UG 5, 11 and broad-band Schott UV-R-280, UV-R-310 or UV-R-340 interference filter depending on the excitation wavelength. The phosphorescence was monitored at right angle to the excitation path with a 0.85 m Spex grating monochromator (model 1402) using narrow slits (between 10/10 μ and 200/200 $\mu \hat{=} 0.1 - 2$ Å band path). A cooled photomultiplier (EMI 9558 QB) was used as a detector. The ODMR apparatus was in principle the same as described by Zuclich et al. [20].

For determining relative radiative rate constants k_i^r, decay rate constants k_i, steady state populations N_i as well as relative intersystem crossing rates s_i (fig. 3) several ODMR techniques were used. Beside the method of slow passage for determining the fine structure parameters D and E we made use of the method of the analysis of phosphorescence transients after a saturating fast passage under continuously exciting conditions as described by Winscom and Maki [21] as well as with flash excitation [22] (Point source Strobex Model 136 Chadwick–Helmuth). Decay rates of dark triplet sublevels were further measured by microwave induced delayed phosphorescence (MIDP)-experiments

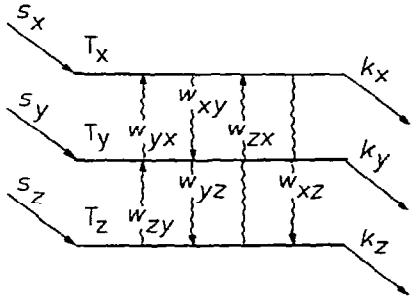

Fig. 3. Dynamic parameters of the triplet sublevels: s_i relative intersystem crossing rates, k_i decay rates and w_{ij} spin lattice relaxation rates.

as described by Schmidt et al. [23] as well as by phosphorescence decay experiments [24]. Because of the large spin–lattice relaxation rates w_{ij} between the triplet sublevels even at 1.3 K, the method of the analysis of the phosphorescence decays during magnetic resonance saturation of sublevels first used by Zuclich et al. [24] was applied for measuring the relaxation free decay rate constants k_i as well as the relaxation rates w_{ij} (fig. 3). For the determination of the relaxation rates w_{ij} the rate equation system describing the population and depopulation of the various levels must be solved [24]. This was done by a Newton–Raphson iteration as described by Co et al. [25], with minor modifications.

Because of the strong intramolecular heavy-atom effect in dibenzothiophene due to the sulphur atom it was possible to detect wavelength dependent population mechanisms in this system. Three excitation possibilities resulting in different steady state populations N_i were observed:

$S_0 \rightarrow S_1$ ($S_1 = 29923\ cm^{-1} \hat{=} 3341.9$ Å) (i)

$S_0 \rightarrow S_2$ ($S_2 \approx 34840\ cm^{-1} \hat{=} 2870$ Å [15]) (ii)

$S_0 \rightarrow T_1$ ($T_1 = 24292\ cm^{-1} \hat{=} 4116.6$ Å). (iii)

The wavelength of the excitation light was 3300 Å for (i) (1/4 m monochromator plus the filters UV-R-340, UG 5, UG 11 and the cutoff filter WG 335), 2800 Å for (ii) (1/4 m monochromator plus the Schott-filter UV-R-280) and 3900 Å for (iii) (1/4 m monochromator plus cutoff filters GG 375 and GG 385).

In the case of the $S_0 \rightarrow T_1$ and the $S_0 \rightarrow S_2$ excitation it was only possible to measure under continuously exciting conditions because of too low intensity of the flash lamp at the corresponding wavelengths.

3. Phosphorescence decay rates

The rate equation for the population of the ith triplet sublevel is given by (see fig. 3)

$$dn_i(t)/dt = s_i - (k_i + w_{ij} + w_{ik})n_i(t) + w_{ji}n_j(t) + w_{ki}n_k(t), \quad (1)$$

with a total decay constant k_i:

$$k_i = k_i^r + k_i^{nr}, \quad (2)$$

where k_i^r is the radiative decay constant and k_i^{nr} the nonradiative decay constant of the sublevel T_i. Under constant irradiation and neglecting SLR processes the steady state condition is given by

$$s_i = k_i N_i, \tag{3}$$

where N_i is the steady state population of the ith sublevel. If one considers the case where the phosphorescence decay is monitored after the exciting light is turned off eq. (1) with $s_i = 0$ is still valid. In the presence of saturating microwave power applied between the jth and kth triplet sublevels during the phosphorescence decay the rate equation is [24]

$$dn(t)/dt = -\tfrac{1}{2}(k_j + k_k + w_{ji} + w_{ki})\, n(t) + \tfrac{1}{2}(w_{ij} + w_{ik})\, n_i(t), \tag{4}$$

where $n_j(t) = n_k(t) = n(t)$. The general solution of the system of the two coupled differential equations (4) and (1) ($s_i = 0$) is given by

$$n(t) = \sum_{n=1}^{2} C_{1n} \exp(-\varphi_n t),$$

$$n_i(t) = \sum_{n=1}^{2} C_{2n} \exp(-\varphi_n t), \tag{5}$$

and the phosphorescence intensity $I(t)$ by a sum of two exponentials

$$I(t) = C \sum_{m,n=1}^{2} k_m^r C_{mn} \exp(-\varphi_n t), \tag{6}$$

where the radiative rate constants are $k_1^r = (k_j^r + k_k^r)$ and $k_2^r = k_i^r$. The decay rates φ_1 and φ_2 are the roots of a quadratic equation [24] and can be observed experimentally. Another independent averaged decay rate $\bar{\varphi}$ can be obtained from the phosphorescence decay in the presence of saturating microwave irradiation between two different pairs of triplet sublevels.

$$\bar{\varphi} = \tfrac{1}{3}(k_x + k_y + k_z). \tag{7}$$

The calculation of all decay rates k_i ($i = x,y,z$) and the SLR-rates w_{ij} ($i,j = x,y,z$) from the observed three pairs of decay constants φ_1, φ_2 and the decay rate $\bar{\varphi}$ is possible [24,25], and this method was used in this paper.

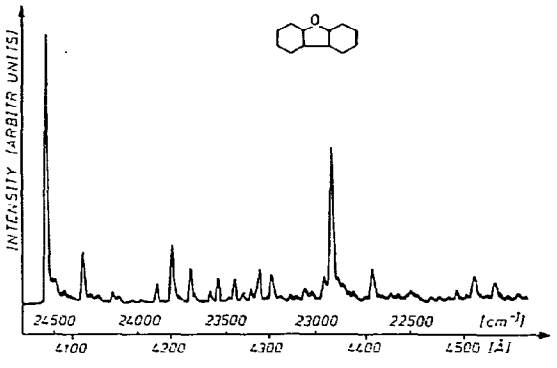

Fig. 4. Phosphorescence emission of X-traps in neat dibenzofuran crystals at 1.3 K.

4. Results

4.1. Phosphorescence

The phosphorescence spectra of all four crystals show very similar vibronic structures. The spectra of the X-traps in neat fluorene and dibenzothiophene crystals are virtual identical to the spectra shown by Bree and Zwarich [9,15]. The phosphorescence spectrum of dibenzofuran is shown in fig. 4 as a typical example.

The phosphorescence spectrum of carbazole is some-

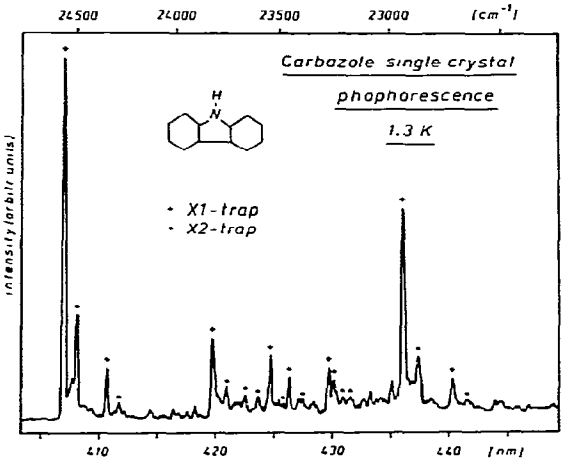

Fig. 5. Phosphorescence emission of X-traps in neat carbazole crystals at 1.3 K (+ X1-trap, • X2-trap).

Table 2
Fluorescence- and phosphorescence 0,0-bands of X-traps in neat fluorene-, carbazole-, dibenzofuran- and dibenzothiophene single crystals

	Fluorescence		Phosphorescence 0,0-band (cm^{-1})
	0,0-band (cm^{-1})	ref.	
fluorene	32834	[44]	23607
carbazole	29322	–	24557 (X_1) 24491 (X_2)
dibenzofuran	32535	[44]	24546
dibenzothiophene	29923	[15]	24292

what more complicated because in carbazole we observed emission from two traps (X1, X2) with a 0–0 band difference of 66 cm^{-1}. Both traps show identical vibronic structure (fig. 5) very similar to that in the spectra of fluorene, dibenzofuran and dibenzothiophene. The linewidth of the vibronic phosphorescence bands is about 2 Å ≙ 12 cm^{-1} for fluorene, carbazole and dibenzofuran. This relatively large linewidth without an indication of phonon structure indicates large inhomogeneous broadening, suggesting a large variety of crystal imperfections. In dibenzothiophene the linewidth of the phosphorescence bands was much smaller, about 0.25 Å ≙ 1.5 cm^{-1}. The nature of the trap in dibenzothiophene is unknown, but the trap is much deeper than in the three other cases. This can be deduced from the fact that dibenzothiophene phosphorescence is still observable at 77 K [15], while in the other three cases no phosphorescence can be observed above 15 K.

In table 2 the wave numbers of the fluorescence and the phosphorescence 0,0-bands are compiled. The 0,0-band of the phosphorescence of fluorene is identical with impurity induced X-trap emission in ref. [9]. The value for dibenzothiophene is the same as found by Bree and Zwarich [15]. The phosphorescence spectrum of dibenzofuran (fig. 4) is very similar to the one found in *n*-heptane [13] but the 0,0-band (24573 cm^{-1}) is shifted 27 cm^{-1} to higher energy. The phosphorescence 0,0-band of the X1-trap in carbazole (24557 cm^{-1}) is 2 cm^{-1} higher than for carbazole in *n*-heptane [10].

Table 3
Triplet zero-field splitting parameters $|D|$ and $|E|$ of fluorene-, carbazole, dibenzofuran- and dibenzothiophene-X-traps in neat crystals as well as $|D|$ and $|E|$ values of fluorene, carbazole, dibenzofuran and dibenzothiophene in low concentration in *n*-heptane at 1.3 K. Error for all values ± 0.0001 cm^{-1}

		$\|D\|$ (cm^{-1})	$\|E\|$ (cm^{-1})
fluorene	X-trap	0.1061	0.0030
	n-heptane	0.1094	0.0036
carbazole	X_1-trap	0.1031	0.0073
	X_2-trap	0.1031	0.0067
	n-heptane	0.1054	0.0067
dibenzofuran	X-trap	0.1073	0.0099
	n-heptane	0.1085	0.0093
dibenzothiophene	X-trap	0.1098	0.0026
	n-heptane	0.1149	0.0024

4.2. Triplet zero field splitting parameters D and E

The triplet zero field splitting parameters $|D|$ and $|E|$ are shown in table 3. In addition the values for low concentration polycrystalline samples in *n*-heptane are given for comparison. With ODMR in zero field only the absolute values of the zero field splitting parameters are observed. From ESR experiments of Behnke [19] we know that the D values have positive signs while the E values have negative signs. As can be seen from table 3, the X1- and X2-trap in carbazole have the same D parameters but slightly different E values. The values of the D parameters in *n*-heptane are all somewhat larger than those of the X-traps, but never more than 5%. The linewidth of the observed ODMR microwave transitions was about 10 MHz for fluorene, carbazole and dibenzofuran, while the linewidth for the X-trap in dibenzothiophene was only 0.8 MHz.

4.3. Dynamic properties

The dynamic properties of the triplet sublevels of fluorene, carbazole, dibenzofuran and dibenzothiophene are compiled in table 4. The values for the energetically lower carbazole X2-trap are shown separately in this

Table 4
Results at 1.3 K. Triplet sublevel decay rates k_i, relative radiative decay rates k_i^r, relative intersystem crossing rates s_i, steady state population N_i and spin lattice relaxation rate w_{ij} of traps in neat crystals of fluorene, carbazole (X1 and X2-trap), dibenzofuran and dibenzothiophene

	Fluorene	Carbazole-X1	Dibenzofuran	Dibenzothiophene	Carbazole-X2
k_x (s^{-1})	0.19 ± 0.02	0.21 ± 0.02	0.21 ± 0.02	3.5 ± 0.2	0.11 ± 0.04
k_y (s^{-1})	0.26 ± 0.02	0.27 ± 0.02	0.31 ± 0.02	2.8 ± 0.2	0.23 ± 0.02
k_z (s^{-1})	0.067 ± 0.005	0.07 ± 0.02	0.13 ± 0.01	0.11 ± 0.01	0.06 ± 0.04
$\bar{\varphi}$ (s^{-1})	0.168 ± 0.006	0.182 ± 0.004	0.213 ± 0.004	2.00 ± 0.15	0.134 ± 0.005
φ_{cal} (s^{-1})	0.172	0.183	0.217	2.13	0.133
k_x^r	0	< 0.1	0.8	58	< 0.1
k_y^r	10	9	14	25.5	15
k_z^r	1	1	1	1	1
s_x (%)	35.5	36.0	36.8	33.6	35.0
s_y (%)	31.9	31.3	31.0	24.8	32.5
s_z (%)	32.6	32.7	32.2	41.6	32.5
N_x (%)	33.6	35.6	37.4	4.7	42.8
N_y (%)	31.7	29.3	29.4	3.1	16.8
N_z (%)	34.7	35.1	33.2	92.2	40.4
w_{xy} (s^{-1})	0.007 ± 0.004	0.003 ± 0.009	0.036 ± 0.006	< 0.3	0.034 ± 0.01
w_{yx} (s^{-1})	0.007 ± 0.004	0.003 ± 0.009	0.035 ± 0.006		0.030 ± 0.01
w_{yz} (s^{-1})	0.048 ± 0.003	0.042 ± 0.006	0.050 ± 0.003	< 0.05	0.088 ± 0.01
w_{zy} (s^{-1})	0.043 ± 0.003	0.038 ± 0.006	0.045 ± 0.003		0.082 ± 0.01
w_{xz} (s^{-1})	0.065 ± 0.009	0.081 ± 0.008	0.102 ± 0.007	< 0.05	0.177 ± 0.01
w_{zx} (s^{-1})	0.057 ± 0.009	0.071 ± 0.008	0.089 ± 0.007		0.156 ± 0.01

table on the right hand side; since the dynamic properties of the triplet sublevels of this X2-trap behave slightly different with respect to the traps in the other molecules they shall be discussed separately.

On top of table 4 are the decay rates k_i shown as they were measured with the method of the analysis of the phosphorescence decay during magnetic resonance saturation of sublevels [24] and described in section 3. In the case of dibenzothiophene the decay rates are given as measured directly by saturating fast passage experiments (k_x, k_y) under continuously exciting conditions [21] as well as by MIDP [23] experiments (k_z, see fig. 6). The latter experiment is in this case more accurate because SLR can be neglected, and we have here two large decay rates and one small rate so that the method of the analysis of the phosphorescence decays during magnetic resonance saturation of sublevels gives a relative large error for the level with the small decay rate. The values found with this method [24] are $k_x = 3.5 \pm 0.2\ s^{-1}$, $k_y = 2.7 \pm 0.3\ s^{-1}$ and $k_z = 0.12 \pm 0.05\ s^{-1}$. Within the given errors the values of both methods agree very well for dibenzothiophene.

There is no agreement between the decay rates of both methods for the other molecules. This is due to the relative large SLR-rates with respect to the decay rates of the sublevels (see end of table 4). If SLR cannot be neglected, the decay k_i^+ of a sublevel i after a saturating fast passage between a single pair of levels i and j under continuously exciting conditions depends in a complicated way on the decay rates k_i, k_j, SLR-rates

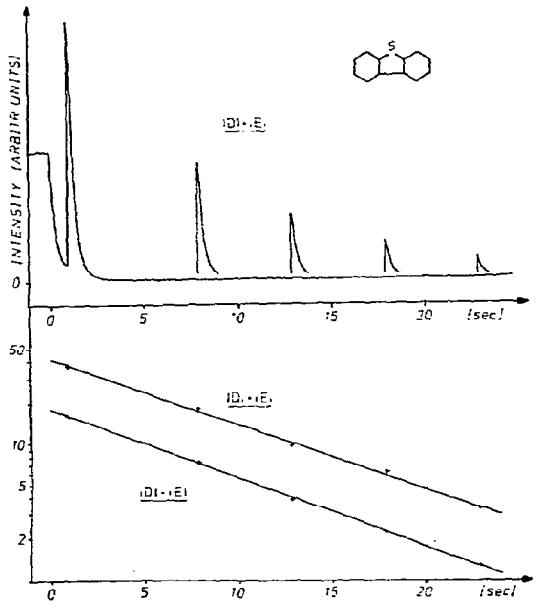

Fig. 6. MIDP experiment on dibenzothiophene X traps at 1.3 K. Top: saturation of the dark z-level and the radiative x-level with different delay times. Bottom: Decay of the dark level taken from $|D|+|E|$ and $|D|-|E|$ transitions by delayed phosphorescence experiments.

w_{ij}, w_{kj} and the intersystem crossing rates s_i and s_j (see eq. (6) in ref. [22]). The measured decay constant k_i^+ after a saturating fast passage is larger than the decay rate k_i. The measured values $\bar{\varphi}$ (eq. (9)) for all molecules are shown in table 4 in the same column as the decay rates k_i. These values were measured by coupling all three triplet sublevels together by simultaneously saturating the transitions between the three levels by a microwave double resonance experiment. This value can be compared with the calculated value $\varphi_{cal} = \frac{1}{3}(k_x + k_y + k_z)$, where the values k_i from table 4 were inserted.

In table 4 are further given the relative radiative rate constants k_i^r and the steady state populations N_i ‡ [21] (error ± 1%) as well as the relative intersystem crossing rates s_i [22] (error ± 1%). The measured steady state populations N_i for fluorene, carbazole and dibenzofuran do not agree with calculated values using the formula $N_i = k_i^{-1} s_i$, which is valid if SLR between the triplet sublevels can be neglected. Only for dibenzothiophene the agreement between measured and calculated N_i is satisfactory. The SLR-rates w_{ij} are given at the end of table 4. For small SLR-rates the errors are relatively high while for the larger relaxation rates the errors are in the range between 10% and 20%. For dibenzothiophene it is only possible to give an upper limit for the SLR-rates.

‡ The measured steady state populations depend very much on the excitation intensity as will be shown later. The values here were measured under conditions where the signal to noise was such that the error of the steady state populations could be estimated to be about 1%.

4.4. Dibenzothiophene

In table 5 the steady state populations are shown as measured under different continuous excitation conditions. The excitation with light of a wavelength of 2800 Å does certainly not result in a pure intersystem crossing from S_2 to T_1 but in a superposition of this process and an internal conversion from S_2 to S_1 followed by intersystem crossing from S_1 to the T_1 state. The second process is probably still the dominant one. Similar observations could be made in phthalazine in a EPA glass [26]. Direct intersystem crossing from $S_0 \rightarrow T_1$ results in a larger population of the middle y-level with respect to the x-level. This larger steady state population in the y-level by $S_0 \rightarrow T_1$ excitation could also be confirmed by detecting a decreasing phosphorescence signal after a saturating fast passage through the 2E transition at this excitation, while in the case of $S_0 \rightarrow S_1$ and $S_0 \rightarrow S_2$ excitation we observed an increasing phosphorescence signal.

Nevertheless at all three excitation wavelengths the z-level contains the main part of the steady state po-

Table 5
Steady state population N_i of the dibenzothiophene trap in neat crystals by different excitations (error ± 1%)

Dibenzothiophene	Excitation		
	$S_0 \rightarrow S_1$	$S_0 \rightarrow S_2$	$S_0 \rightarrow T_1$
N_x	4.7%	9.4%	5.7%
N_y	3.1%	4.9%	7.9%
N_z	92.2%	85.7%	86.4%

pulation. Because this level has a long lifetime and is only very little radiative with respect to the two other levels, large signals can be observed by MIDP experiments [23]. In fig. 6 are shown on top the signals of such an experiment at different delay times after a saturating fast passage through the $|D|+|E|$ transition. The observed decay time of the z level (9.0 s) can be taken from the plot of the lower part of fig. 6, where the height of the MIDP-signals is plotted against the delay times from the $|D|+|E|$ and $|D|-|E|$ transitions. In both cases we find very good exponential decays for the z level.

5. Discussion

We assume that the observed X-trap molecules are mainly due to lattice imperfections and not due to impurity induced traps, because of the low impurity concentration range of 5–50 ppm (see appendix) for all investigated neat single crystals of the four hydrocarbons. This assumption is supported by experiments on mixed crystals of dibenzofuran and fluorene [36] which showed from the phosphorescence intensity ratio of trap and guest molecule emission that the concentration of X-traps in the neat crystals should be larger than 1000 ppm. All here reported results were obtained on such X-trap molecules in neat single crystals.

5.1. Dynamic properties

The dynamic parameters of the triplet sublevels of fluorene, carbazole X1, dibenzofuran and dibenzothiophene give an uniform picture and will be discussed together. The changes in the decay rates k_i from fluorene to dibenzofuran due to the somewhat heavier nucleus O instead of C is very small. This was expected not only because of the small difference in the atomic number of C, N and O in fluorene, carbazole and dibenzofuran but also because of the lower spin density at the 9 position. The measured $\bar{\varphi}$ value is about 25% larger for dibenzofuran, with respect to fluorene. For dibenzothiophene a drastic change due to the intramolecular heavy-atom effect of the S nucleus can be noticed. The $\bar{\varphi}$-value is larger by about a factor ten than for dibenzofuran. Looking at the decay rates we see that especially the in plane levels x and y are affected by the intramolecular heavy-atom effect, while the out of plane z-level is not affected at all. This can also be seen from the relative radiative rate constants k_i^r. In fluorene, carbazole and dibenzofuran the y-level is the most radiative one. In fluorene the x-level decays only radiationless, while in carbazole this level radiates very little and in dibenzofuran nearly as strong as the z-level. In dibenzothiophene this x-sublevel is the most radiative one. This shows that the intramolecular heavy-atom effect due to the sulphur atom is selective and affects mainly the radiative decay rates [27].

The relative intersystem crossing rates s_i are similar for all three triplet sublevels in fluorene, carbazole X1 and dibenzofuran. There is no large selectivity but the x-level has with about 36% the largest relative intersystem crossing rate while the y- and z-levels have nearly the same rates. In the case of dibenzothiophene the largest relative intersystem crossing rate is s_z with about 42%. That means the intramolecular heavy-atom effect seems to affect mainly the z-level with respect to the intersystem crossing process from the first excited singlet state S_1 to the triplet state T_1, but mainly the x- and y-levels with respect to the decay process from T_1 to the singlet ground state S_0. The same conclusion follows from the observed steady state populations N_i by different excitation processes (table 5).

5.2. Spin–lattice relaxation

Data about SLR-rates in the excited triplet state of organic molecules in crystals are very rare. Fischer and Denison [28] and Schwoerer and Sixl [29] first measured SLR-rates in the triplet state of organic molecules using ESR techniques. In zero field Hall and El-Sayed [30] determined relaxation rates by adjusting a sum of three exponentials to the decay of the phosphorescence intensity. Zuclich et al. [24] simplified the method by generating a quasi-two level system via continuous saturating of one of the zero field transitions with a resonant microwave field. Winscom et al. [31] reported a method of determining SLR-rates in the limit of "fast" SLR at 77 K. Antheunis et al. [32,33] have developed a method for measuring SLR-rates under continuous illumination.

Considering the measured relaxation rates w_{ij} for fluorene carbazole and dibenzofuran it can be seen that the relaxation among the triplet sublevels is markedly anisotropic. This result is in agreement with measurements done on other molecules [24,25,32]. For all

traps the largest SLR-rate is observed between the x- and z-levels corresponding to the $|D| + |E|$ splitting, while the smallest SLR-rate belongs to the corresponding $2|E|$ splitting.

This observation is in qualitative agreement with measurements of Winscom and Dinse [34] done in the limit of "fast" SLR at 77 K on diazaaromatic molecules. These authors could show that the SLR-rates are proportional to the square of the energy splitting of the triplet sublevels due to reorientation of the spin axes by a small angle of about 1° in a thermally populated triplet state. In the case of fluorene, carbazole and dibenzofuran at 1.3 K it seems that the SLR-rates show the same behaviour [34] but in addition there is a small constant SLR-rate superimposed.

For dibenzothiophene only an upper limit can be given for the SLR-rates. Because the decay rates k_x and k_y are relatively large, the upper limit for w_{xy} and w_{yx} cannot be smaller than 0.3 s^{-1}.

The decay experiments after the light was turned off showed some discrepancies between the results of experiments under continuously exciting conditions. Comparing the decays k_i and the SLR-rates of table 4 with the observed decays after a saturating fast passage we have reason to assume that the SLR-rates under continuously exciting conditions are clearly larger than under conditions where the light is turned off. From eq. (6) in ref. [22] we can estimate the decay rate after a saturating fast passage in the presence of SLR. The measured decay constant k^+ after a $|D| - |E|$ or $2|E|$ transition under continuously exciting conditions are about twice as large as the estimated value. (For dibenzofuran we measured a decay $k_y^+ = 0.92$ s^{-1} under these conditions; see fig. 7, bottom.) This can have mainly the reason, that spin lattice relaxation rates could become more significant by some heating of the sample caused by the exciting light as pointed out in refs. [24,33]. Therefore the following experiment was done (see fig. 7). Measuring the height of the signal ΔI after a saturating fast passage devided by the steady state phosphorescence I_0 versus the excitation intensity, a plot was obtained as shown on top of fig. 7 (dibenzofuran after saturating the $2|E|$ transition). At lower excitation intensity the spin polarisation is much higher between the x- and y-level, very similar to a value which can be calculated from the measured intersystem crossing rates, showing that the SLR rates become smaller with lower excitation itensity. We expected now to find a much smaller decay rate for the fast passage decay at small excitation intensity, but the observed decay rate was only about 10% smaller as for high excitation intensities. Therefore we assume that an additional process is important for the decay after a saturating fast passage under continuously exciting conditions, which was described by Fayer and Gochanour [35] and which should be specially important for shallow traps as in our neat crystals fluorene, carbazole and dibenzofuran.

In general the exciton spin sublevels will have decay rates which are different from those of the shallow traps. An exchange of population between the exciton band and the trap will result in trap decay rates which are weighted averages of the exciton band and the trap decay rates, where the weighting factor is determined by the probability of finding an excitation in the trap. For larger decay rates of the exciton band with respect to the trap decay rates, this process leads to the fact that the measured decay rates k_i^+ for the decay after a saturating fast passage are larger than the values k_i given in table 4. The reason that we do not observe this process in the case of the dibenzothiophene trap is due to the fact that this special type of trap is much deeper than the traps in the three other molecules and there-

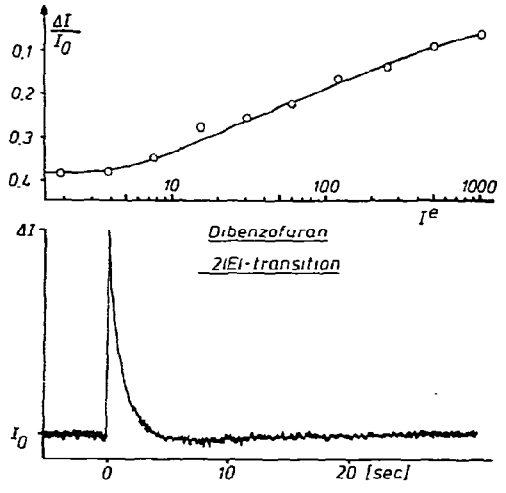

Fig. 7. ODMR-fast passage signal of the $2|E|$-transition of dibenzofuran X traps (bottom) and dependence of the signal height ΔI with respect to the steady state phosphorescence intensity I_0 on the excitation intensity I^e.

fore the exchange between the exciton band and the trap is obviously much slower.

The shallow traps in fluorene, carbazole and dibenzofuran seem to be typical examples to prove the described mechanism of rapid exchange of population between the exciton band and the trap [35].

5.3. X2-trap in Carbazole

The results of the X2-trap in carbazole are much less accurate than those for the other X-traps. The main reason are the relative large SLR-rates, especially between the x- and z-levels, resulting in very similar decay rates k_x^+ and k_z^+ equal to $0.067 \pm 0.003\ s^{-1}$ from MIDP experiments (here k_i^+ is used for the measured decay rate, which is composed of the decay rate k_i and the SLR rates w_{ij} (see eq. (6) ref. [22])). This shows that the x- and z-levels are strongly coupled by SLR and therefore the analysis of the phosphorescence decays during magnetic resonance saturation of sublevels [24] is very inaccurate. Nevertheless, within the error limits the decay rates k_y and k_z of the X1- and X2-trap are very similar, while k_x of the X2-trap is much smaller than k_x for the X1-trap. This smaller k_x rate is also reflected in the measured $\bar{\varphi}$ value for the 66 cm^{-1} energeticly lower X2-trap.

For comparison, carbazole in low concentration in n-heptane was measured. At 1.3 K SLR could be neglected in this case. The measured decay rates $k_x = 0.11\ s^{-1}$, $k_y = 0.25\ s^{-1}$ and $k_z = 0.06\ s^{-1}$ agree very well with the decay rates of the X2-trap. The larger k_x rate for the shallower X1-trap might be due to an additional depopulation of this top level into the exciton band.

6. Conclusions

The investigations on the triplet state of the shallow X-traps in neat crystals of fluorene, carbazole and dibenzofuran have shown a very similar dynamic behaviour of the triplet sublevels of the three molecules. The observed SLR-rates at 1.3 K between the triplet sublevels have the same order of magnitude as the decay rates. A rapid exchange of population between the exciton band and the shallow X-traps seems to be an important mechanism. The traps in neat dibenzothiophene crystals show a different dynamic behaviour of the triplet sublevels with respect to the three other molecules. This is due to a strong intramolecular heavy-atom effect of the sulphur atom, which even allows a direct effective $S_0 \rightarrow T_1$ excitation.

Fluorene, carbazole, dibenzofuran and dibenzothiophene of sufficient purity are interesting materials as host matrices for optical investigations in mixed crystals with low guest concentrations. Furthermore fluorene and dibenzofuran as well as dibenzofuran and dibenzothiophene form solid solutions. So fluorene and dibenzofuran can be mixed at any suitable percentage up to 50 : 50% [36], forming one of the rare molecular mixed crystal systems with high guest concentrations which is not an isotopic mixed system, and therefore very useful for the study of dimer-, trimer- and higher aggregate electronic states.

Acknowledgement

We thank Professor K.H. Hausser for his special interest in this work and for helpful discussions. We also thank Dr. K.P. Dinse and Dr. U. Haeberlen for critical reading and discussing the manuscript. We wish to express our gratitude to Mrs. Gudrun Pampel, University of Stuttgart, for the GLC measurements.

Appendix

A.1. Fluorene

Commercial fluorene isolated from coal tar was found to contain, beside the main impurity anthracene, small amounts of structurally related impurities like 5,6-benz-f-indane [37]. These are not easily separated by recrystallisation or zone refining techniques. In fact, Bree and Zwarich [38] developed a tedious purification scheme for removing the various impurities. Similarly it was suggested that fluorenone can be synthesized from fluorene-9-carboxylic acid [39] by treatment of the acid with $Na_2Cr_2O_7$, followed by two subsequent reduction steps: first with zinc/ammonia to fluorenole, then by Clemmensen reduction or with HJ/phosphorous to the fluorene. This product contains among other impurities the by-product 9,9'-bifluorenyl. Therefore we looked for a method to synthesize fluorene where we were able to purify the starting compound to large extend and where we could avoid forming im-

purities during the reduction of fluorenone: diphenyl-2-carboxylic acid, either prepared by carboxylation at 2-diphenylmagnesiumiodide [40] or as commercially available (Koch–Light Lab.) was purified by repeated treatment with potassiumhydroxide, extraction with diethylether and acidification with HCL. It was cyclised to fluorenone with H_2SO_4 and reduced in ethylenglycole via the Wolff–Kishner method to fluorene in high yield and purity. After two subsequent sublimations and horizontal zone refining (200 passes), the fluorene was analysed by GLC and showed total impurities of the order of 10–50 ppm

Experimental

Diphenyl-2-carboxylic acid (38 gr) and H_2SO_4 (200 gr) were heated with stirring for half an hour at exactly 80°C. The deeply coloured solution was poured into ice. The fluorenone was isolated, made alkaline and repeatedly extracted with diethylether. The combined ether solutions were washed and dried, yielding after evaporation 95% fluorenone.

Fluorenone (30 gr), ethylenglycole (750 ml) and hydrazinhydrate (80 ml) were refluxed for 6 h, while the fluorene was azeotropically carried out of the reaction mixture. It solidified out in the reflux condenser, from which it was worked off with diethylether. It was acidified with HCL, extensively washed with water and dried with anhydrous Na_2SO_4. Evaporation under reduced pressure yielded 23 gr fluorene.

A.2. Dibenzofuran

Commercial dibenzofuran contains up to 5% fluorene which cannot be removed by zone-refining, as these two substances have the interesting property of forming together a solid solution. This property, as pointed out by Lüttringhaus and Hauschild [41], is apparent from the melting point and solidification data at various concentrations. These workers found the isomorphic substitution of fluorene in dibenzofuran. They therefore suggested the preparation of dibenzofuran from extensively purified ortho-diphenole: dehydration with zincchloride yields fluorene-free dibenzofuran. We found this synthesis is the most suitable one for single crystal studies.

Experimental

2.2′-dihydroxybiphenyl was dissolved in dilute potassiumhydroxid solution and washed three times with diethylether. This was followed by acidification and recrystallisation from water. This purified material (30 gr) and zincchloride (90 gr) were heated and stirred together. The temperature was raised over a 45 min period to 250°C and maintained for 1.5 h. The dibenzofuran was then distilled off under reduced pressure. Extraction with diethylether/sodium hydroxide solution, evaporation and subsequent recrystallisation from methylalcohol (three times), yielded dibenzofuran in 75–80% yield. GLC analysis at the dibenzofuran showed total impurities to be less then 20 ppm. No fluorene or anthracene was detected.

A.3. Carbazole

Commercial carbazole is isolated from the crude anthracene fraction of coal tar. It therefore, contains various amounts of impurities such as anthracene and phenanthrene. We found that "pure" carbazole, useful for molecular crystals, is best prepared synthetically by a single step reduction of 2-nitrobiphenyl with triethylphosphit. This is described by Cadogan et al. [42]. The commercially available starting material is first carefully purified. GLC after extensive zone refining of the so obtained carbazole, showed the total impurity concentration to be on the order of 10–400 ppm. Clearly, the impurity concentration was a function of which portion of the zone refining tube the sample was taken.

A.4. Dibenzothiophene

Dibenzothiophene was synthesized in accordance with a method outlined in the patent literature [43]. Highly purified diphenyl reacts with elemental sulfur and $AlCl_3$ as catalyst to give the desired product.

Experimental

Diphenyl (61 gr) and elemental sulfur (26 gr) were melted together at 115–120°C. $AlCl_3$ (3 gr, highly pulverized) was added over 30′. The temperature was then maintained for additional 2.5 h. It was then in-

creased during a period of 8–10 h to 240°C. The dibenzothiophene was distilled out under reduced pressure, recrystallized three times from boiling alcohol and finally zone refined. GLC analysis showed impurity traces in the concentration range at 5–50 ppm.

Notes

The GLC was a Varian 1520 equipped with solid state injection system, carbowax 20 M or XE 60 5% on chromosorb W, isothermal heating. Column temperatures: fluorene and dibenzofuran 160°C, dibenzothiophene 150°C and carbazole 180°C. Carrier gas nitrogen, FID.

All crystals used were grown from the melt. The crystals were slowly (10°C/day) cooled to room temperature.

References

[1] A. Proepstl and H.C. Wolf, Z. Naturforsch. 18a (1963) 724.
[2] M. Schwoerer and H.C. Wolf, Proc. XIVth Coll. Ampere 1966, Ljubljana, ed. R. Blinc. (North-Holland, Amsterdam, 1967) p. 544; Mol. Crystals 3 (1967) 177.
[3] R.M. Hochstrasser and D.S. King, J. Am. Chem. Soc. 97 (1975) 4760.
[4] D.M. Burns and J. Iball, Proc. Roy. Soc. A227 (1955) 200.
[5] B.M. Lahiri, Z. Krist. 127 (1968) 456.
[6] O. Dideberg, L. Dupont and J.M. André, Acta Cryst. B28 (1972) 1002.
[7] M. Schaffrin and J. Trotter, J. Chem. Soc. A (1970) 1561; A. Bree and R. Zwarich, Spectrochim. Acta 27A (1971) 599.
[8] A. Bree and R. Zwarich, J. Chem. Phys. 51 (1969) 903.
[9] A. Bree and R. Zwarich, J. Chem. Phys. 49 (1968) 3344.
[10] H.J. Haink and J.R. Huber, J. Mol. Spectry. 60 (1976) 31.
[11] M. Tanaka, Bull. Chem. Soc. Japan 49 (1976) 3382.
[12] A. Bree and V.V.B. Vilkos, J. Mol. Spectry. 48 (1973) 124.
[13] A. Bree and V.V.B. Vilkos, J. Mol. Spectry. 48 (1973) 134.
[14] A.R. Lacey, A.E.W. Knight and I.G. Ross, J. Mol. Spectry. 47 (1973) 307.
[15] A. Bree and R. Zwarich, Spectrochim. Acta 27A (1971) 621.
[16] H. Sixl and H.C. Wolf, Z. Naturforsch 27a (1972) 198.
[17] V. Zimmermann, M. Schwoerer and H.C. Wolf, Chem. Phys. Letters 31 (1975) 401.
[18] V. Zimmermann, H.C. Wolf and M. Schoerer, Chem. Phys. Letters 31 (1975) 406.
[19] J. Behnke, Ph.D. Thesis, Universität Heidelberg, Germany (1975).
[20] J. Zuclich, D. Schweitzer and A.H. Maki, Photochem. Photobiol. 18 (1973) 161.
[21] C.J. Winscom and A.H. Maki, Chem. Phys. Letters 12 (1971) 264.
[22] D. Schweitzer, J. Zuclich and A.H. Maki, Mol. Phys. 25 (1973) 193.
[23] J. Schmidt, W.S. Veeman and J.H. van der Waals, Chem. Phys. Letters 4 (1969) 341.
[24] J. Zuclich, J.U. von Schuetz and A.H. Maki, Mol. Phys. 28 (1974) 33.
[25] T. Co, R.J. Hoover and A.H. Maki, Chem. Phys. Letters 27 (1974) 5.
[26] Y.H. Li and E.C. Lim, J. Chem. Phys. 56 (1972) 1004.
[27] G. Giachino and D.R. Kearns, J. Chem. Phys. 53 (1970) 3886.
[28] P.H.H. Fischer and A.B. Denison, Coll. Ampere (1968) Ed. P. Averbuch (1969) p. 455; Mol. Phys. 17 (1969) 297.
[29] M. Schwoerer and H. Sixl, Z. Naturforsch. 24a (1969) 952.
[30] L.H. Hall and M.A. El-Sayed, J. Chem. Phys. 54 (1971) 4958; Chem. Phys. 8 (1975) 272.
[31] C.J. Winscom, K.P. Dinse and K. Möbius, Proceeding of the XIXth Congress Ampere, Heidelberg, 1976, eds. H. Brunner, K.H. Hausser and D. Schweitzer, Groupement Ampere Heidelberg–Geneva.
[32] D.A. Antheunis, B.J. Botter, J. Schmidt, P.J.F. Verbeek and J.H. van der Waals, Chem. Phys. Letters 36 (1975) 225.
[33] D.A. Anthenis, Ph.D. Thesis, University of Leyden, The Netherlands (1974).
[34] C.J. Winscom and K.P. Dinse, Spring Meeting of the DPG München, 1978;
K.P. Dinse, private communications.
[35] M.D. Fayer and G.R. Gochanour, J. Chem. Phys. 65 (1976) 2472.
[36] D. Schweitzer and H. Zimmermann, to be published.
[37] E.A. Johnson, J. Chem. Soc. (1962) 994.
[38] A. Bree and R. Zwarich, Spectrochim. Acta 25A (1969) 713.
[39] Y. Kanda, R. Shimada, K. Hanada and S. Kajigaeshi, Spectrochim. Acta 17 (1961) 1268.
[40] A.S. Harris, E.N. White and D. McNeil, J. Chem. Soc. (1955) 4216.
[41] A. Lüttringhaus and K. Hauschild, Chem. Ber. 73 (1940) 145.
[42] J.I.G. Cadogan, U. Cameron-Wood, R.M. Mackie and R.J.G. Searle, J. Chem. Soc. (1965) 4831.
[43] German Patent No. 579917 (1931).
[44] H. Schneckenburger, Diplomarbeit, Universität Stuttgart, Germany (1976).